

Supporting information

Intrinsic Viscosity of Cyclic Polystyrene

Youncheol Jeong, Ye Jin, Taihyun Chang*

Division of Advanced Materials Science and Department of Chemistry,
Pohang University of Science and Technology (POSTECH), Pohang, 37673, Korea

Filip Uhlik

Department of Physical and Macromolecular Chemistry,
Charles University, Prague, 12843, Czech Republic

Jacques Roovers

Institute for Environmental Chemistry,
National Research Council of Canada, Ottawa, Canada

Figure S1. A part of the simulation trace for R_g^2 for a polymer chain with 1000 beads. The ensemble average is shown as a line.

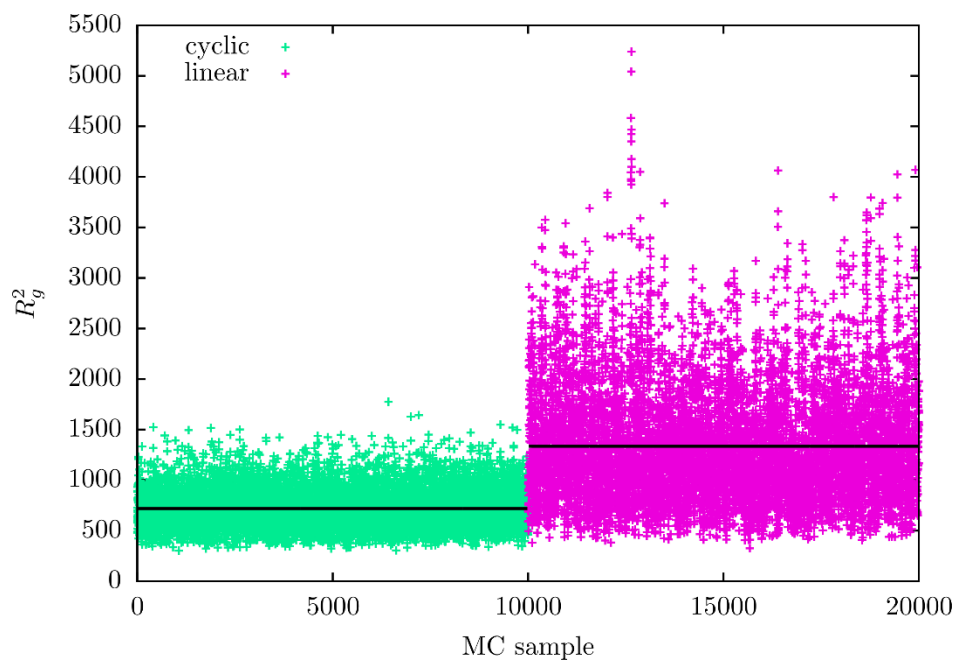


Figure S2. A part of the simulation trace for $[\eta]$ for a polymer chain with 1000 beads. The ensemble average is shown as a line.

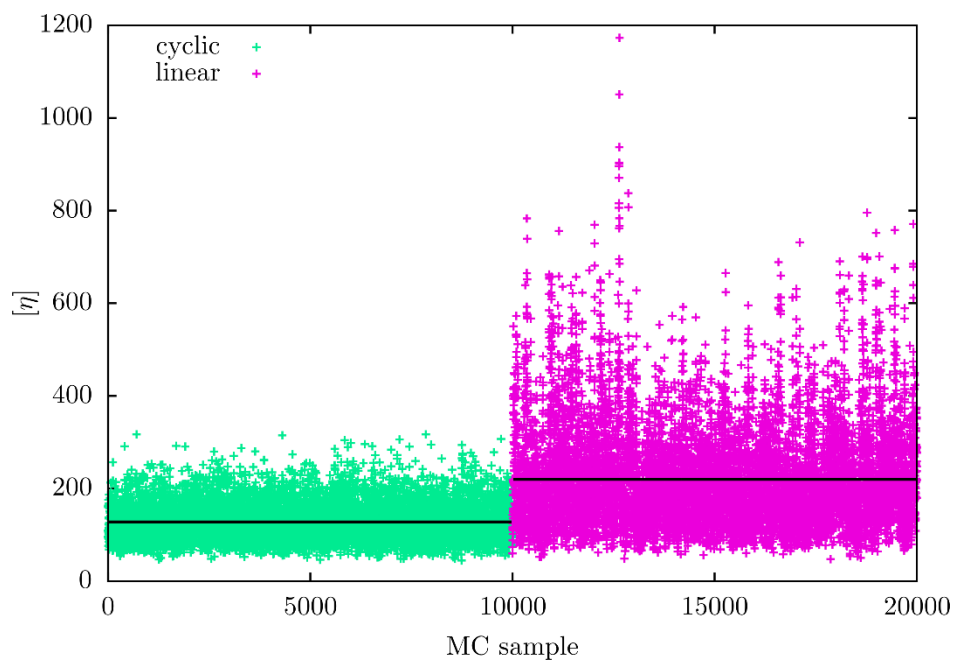


Figure S3. A simulation snapshot of cyclic polymer with 1000 beads with radius of gyration close to the ensemble average.

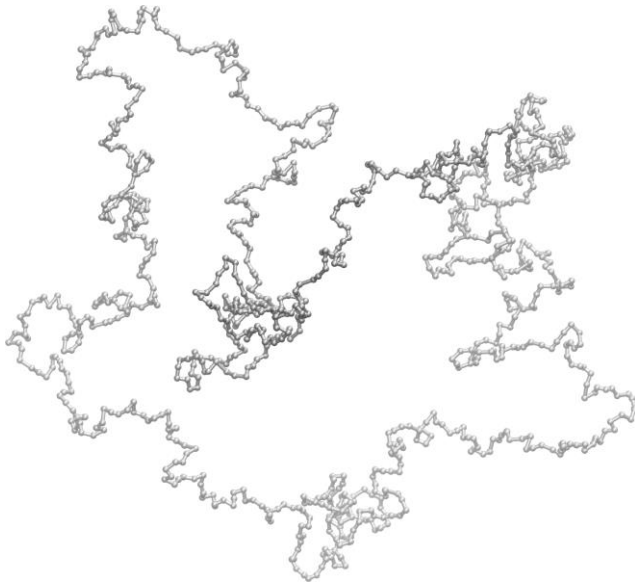


Figure S4. A simulation snapshot of linear polymer with 1000 beads with radius of gyration close to the ensemble average.

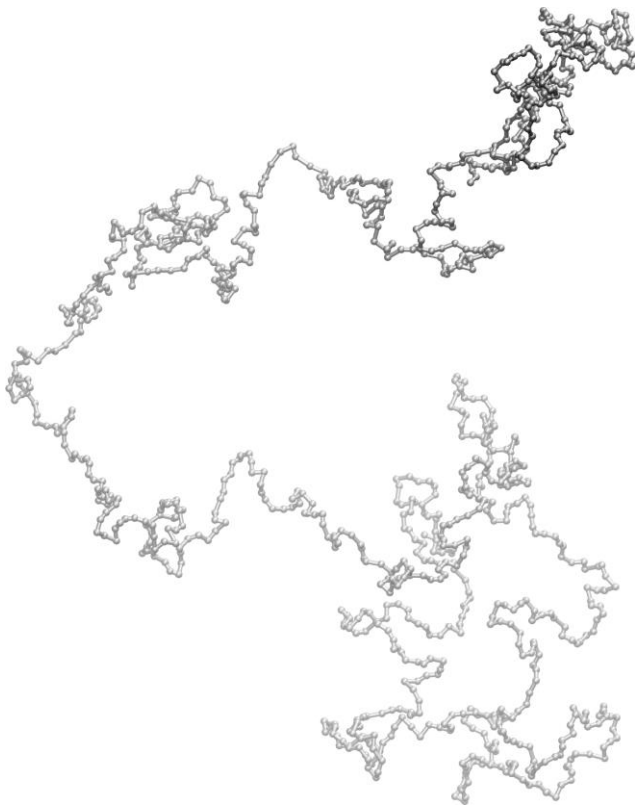


Figure S5. log MW vs. elution time plot of C-PS and L-PS in the SEC analysis. C-PS and L-PS show parallel lines and the shift yields the relationship, $MW_{C, App} = 0.72 MW_L$.

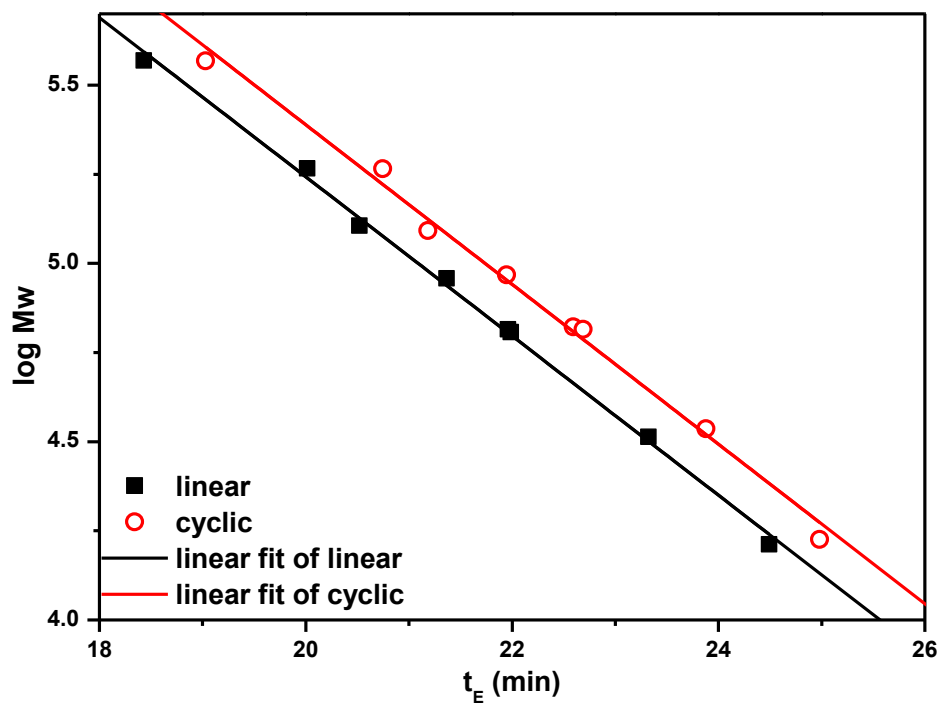
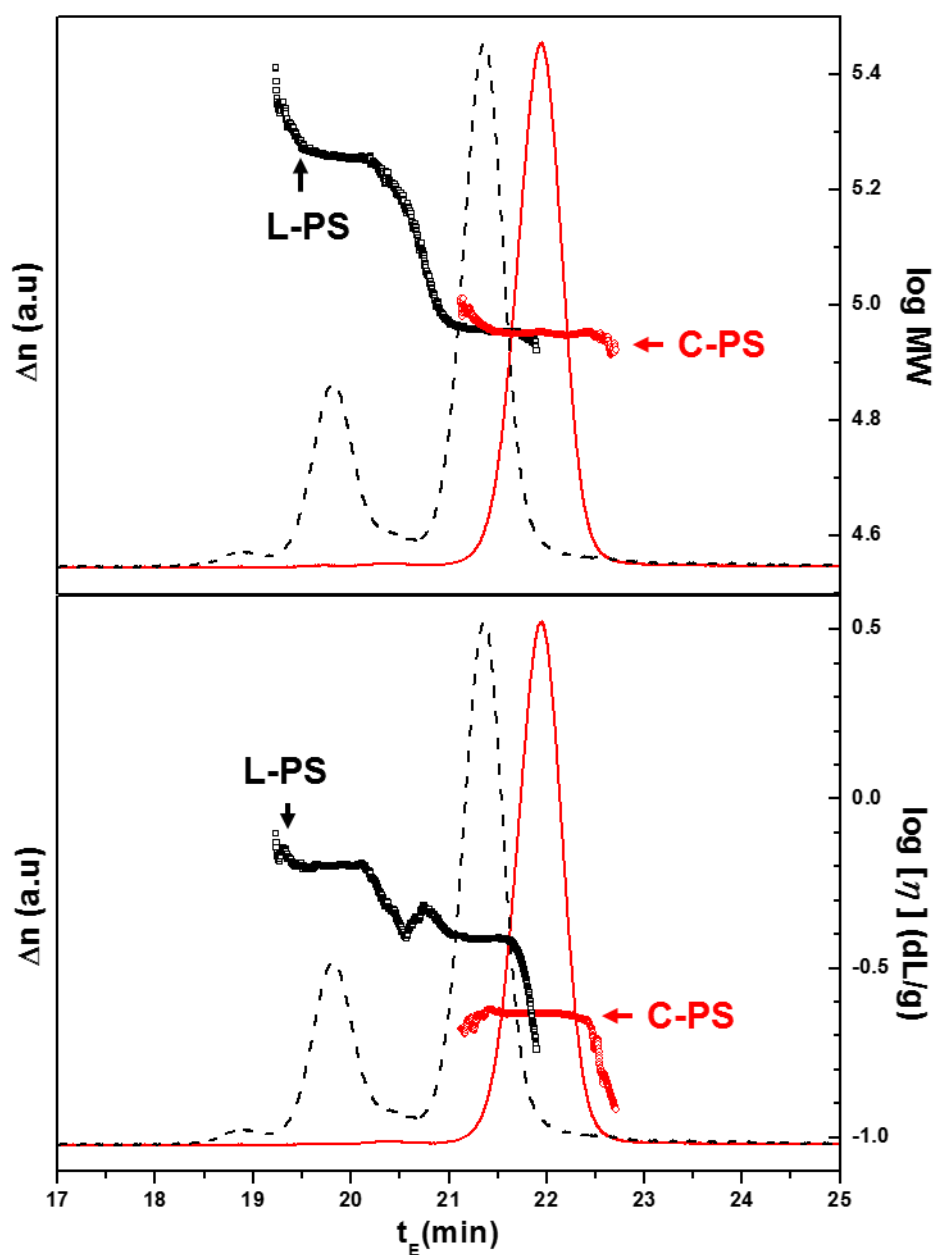
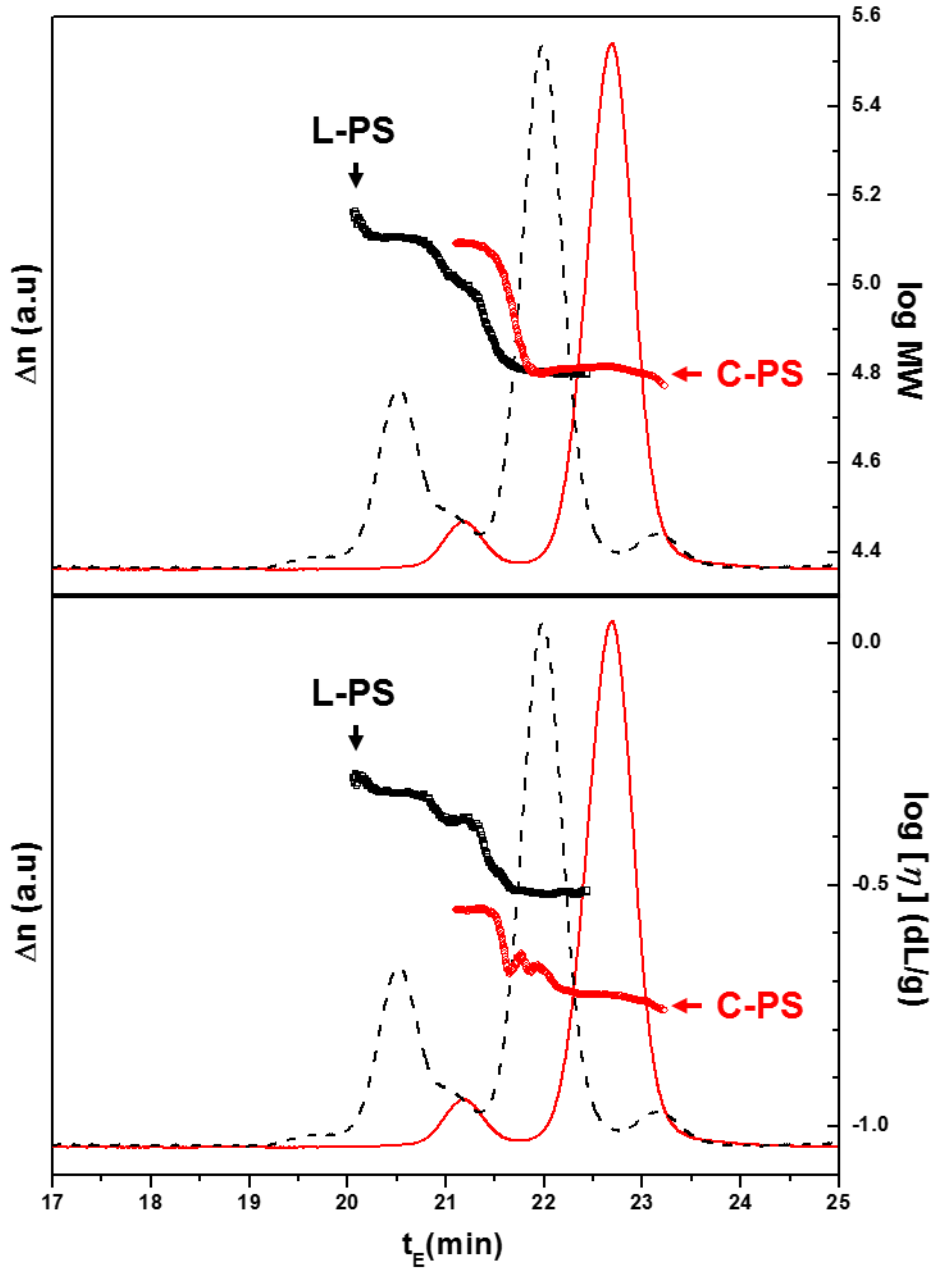


Figure S6. SEC chromatograms of the series of C-PS parts (red solid line) and the L-PS parts (black dotted line) recorded by RI detector. The molecular weight obtained from the LS detection (top) and the intrinsic viscosity obtained from the viscometer detection (bottom) are shown in the plot. SEC condition: three PS/DVB columns (Agilent Polypore 300 × 7.5 mm, Waters Styragel HR4 300 × 7.8 mm, and Jordi mixed bed 300 × 8.0 mm) were used with THF eluent at a flow rate of 0.7 mL/min.

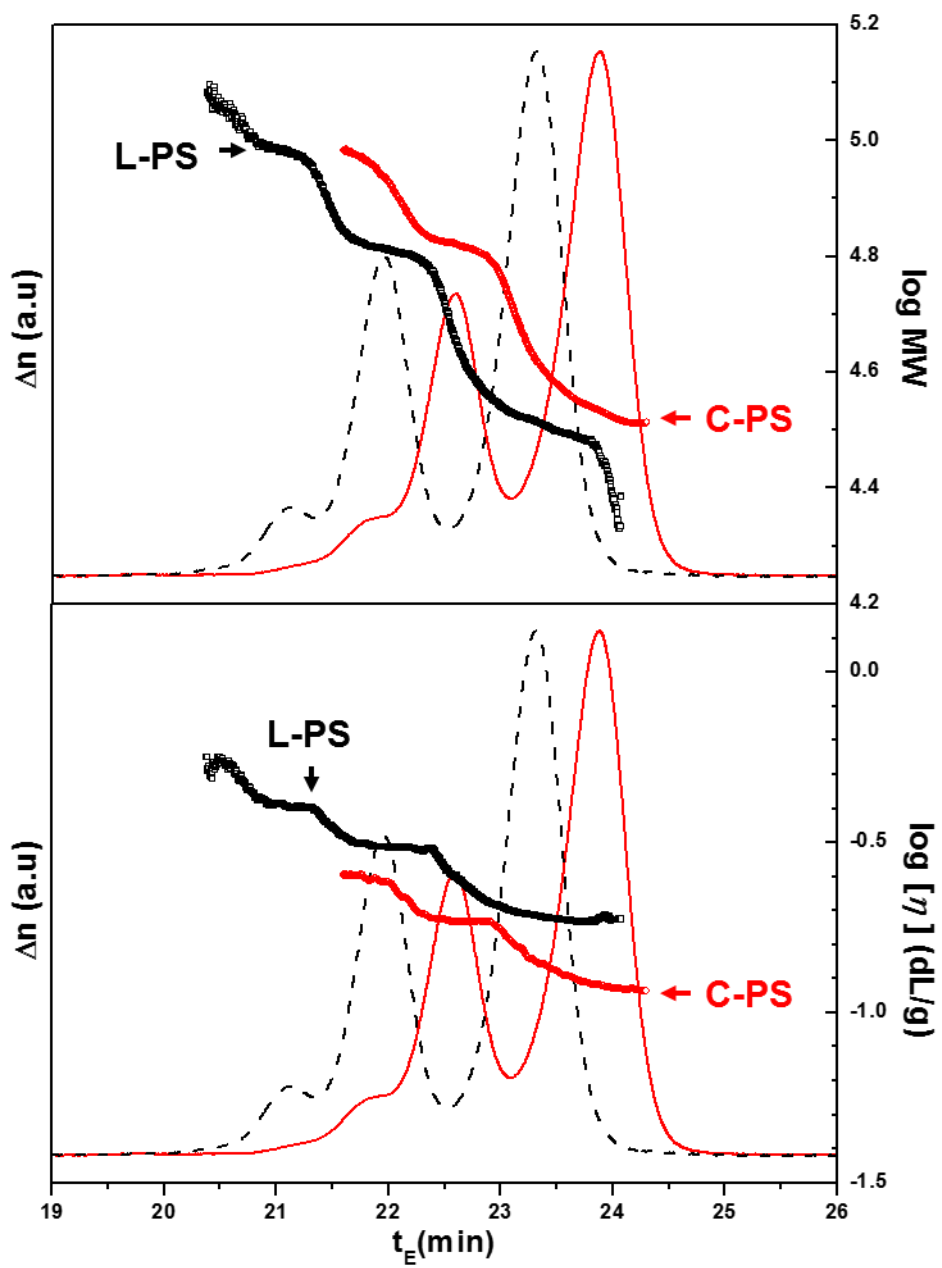
C-PS 4 part and L-PS 4 part



C-PS 3 part and L-PS 3 part



C-PS 2 part and L-PS 2 part



C-PS 1 part and L-PS 1 part

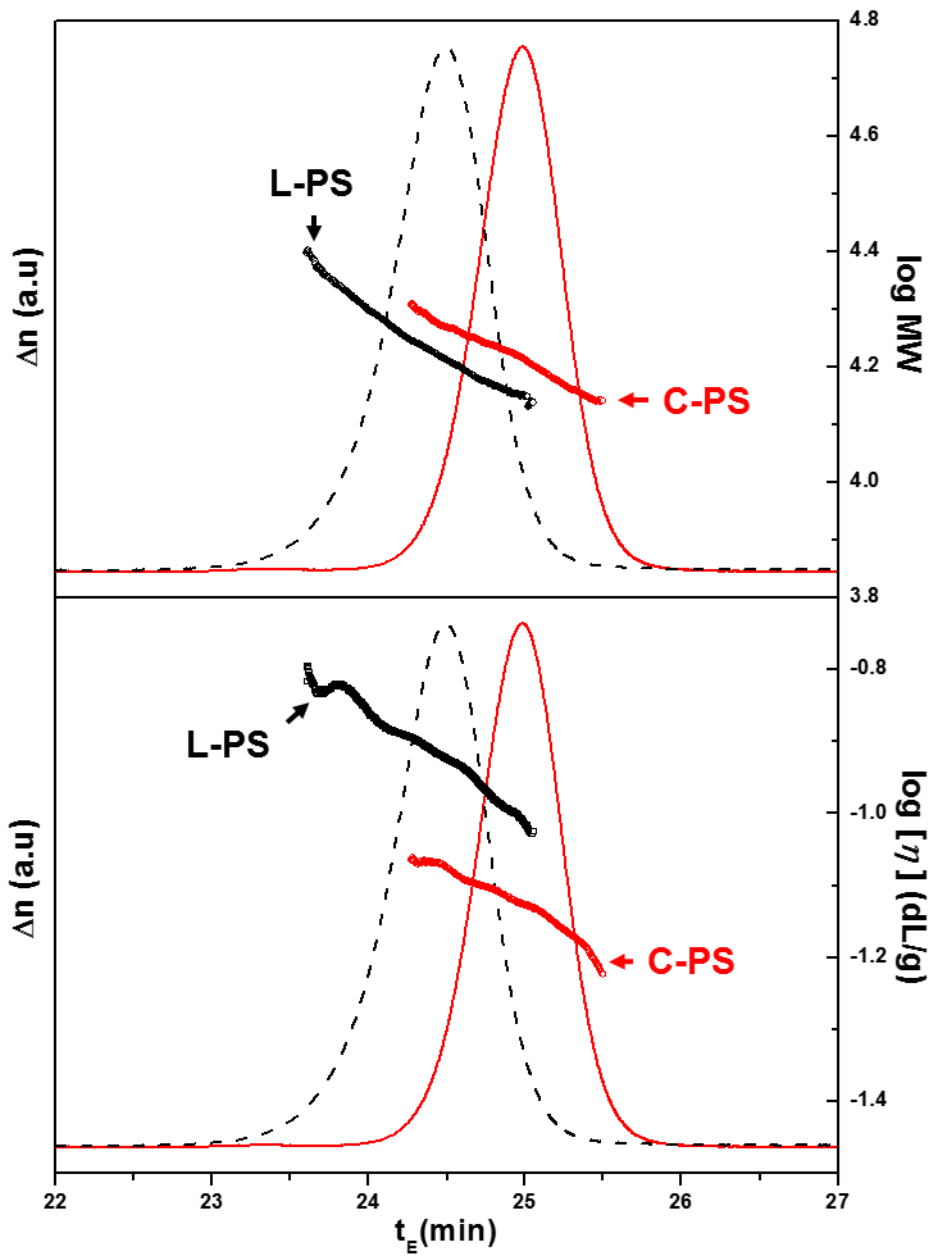


Table S1. Molecular weights and intrinsic viscosities of fractionated L-PS and C-PS samples.

Sample	M_p^a	$[\eta]_L$ (dL/g) ^b	Sample	M_p^a	$[\eta]_C$ (dL/g) ^b
L-PS 1	16.3k	0.12 ₀	C-PS 1	16.8k	0.07 ₉
L-PS 2	32.6k 65.3k	0.19 ₇ 0.32 ₄	C-PS 2	34.4k 66.4k	0.12 ₇ 0.19 ₀
L-PS 3	64.1k 127.5k	0.32 ₁ 0.51 ₂	C-PS 3	65.3k 123.7k	0.19 ₂ 0.29 ₄
L-PS 4	90.7k	0.41 ₁	C-PS 4	92.8k	0.24 ₇
L-PS 5	184.5k 370.8k	0.66 ₂ 1.07 ₄	C-PS 5	184.2k 369.5k	0.38 ₆ 0.61 ₉

^a Determined by SEC/Light scattering in THF.

^b Determined by SEC/Viscometer at M_p in THF at 25°C.

Figure S7. Universal calibration of C-PC and L-PS.

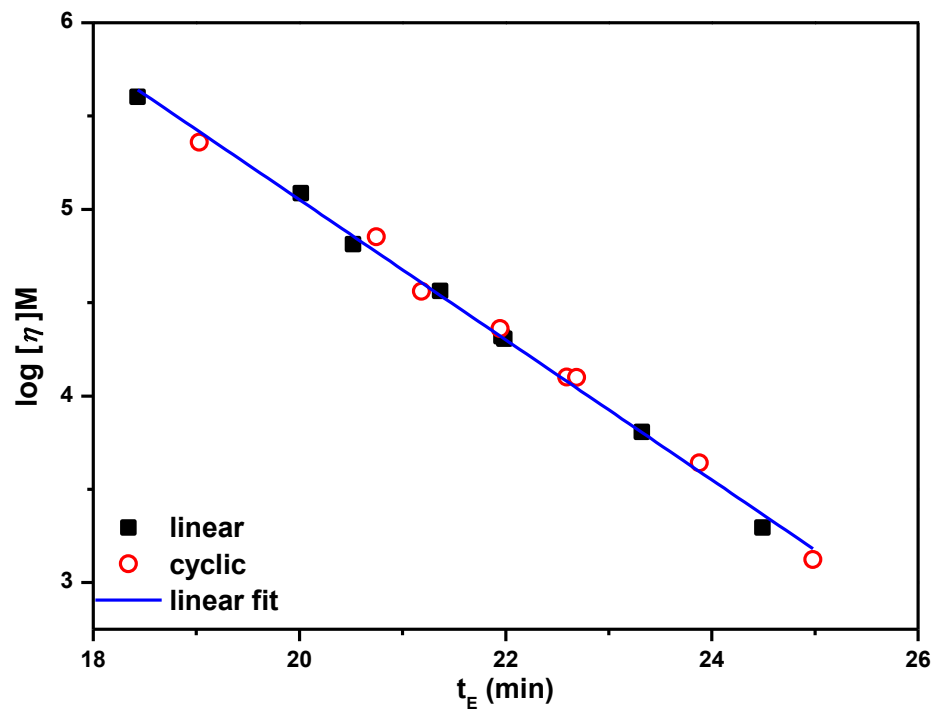


Figure S8. The dependence of the squared radius of gyration on the number of beads. The limiting slopes of linear and cyclic polymers at high N are the same, 1.20.

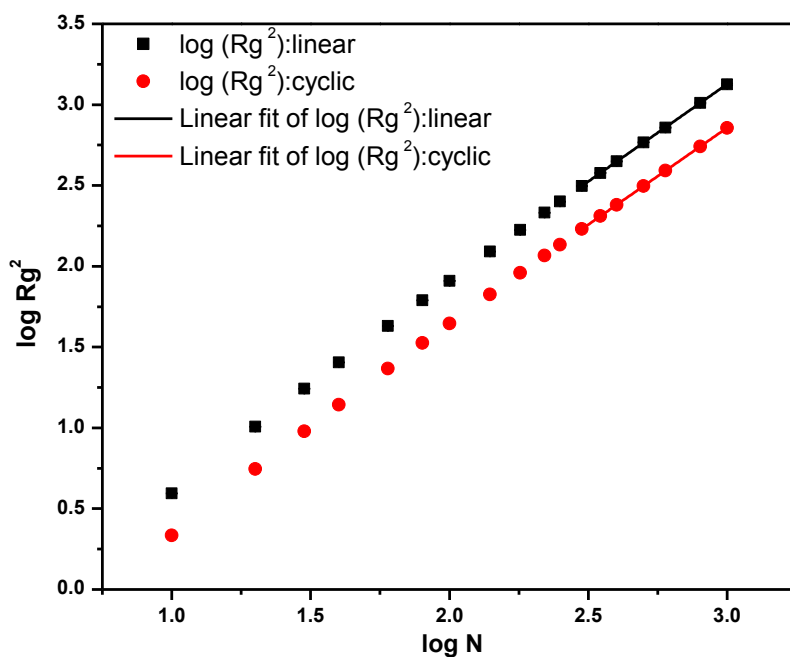
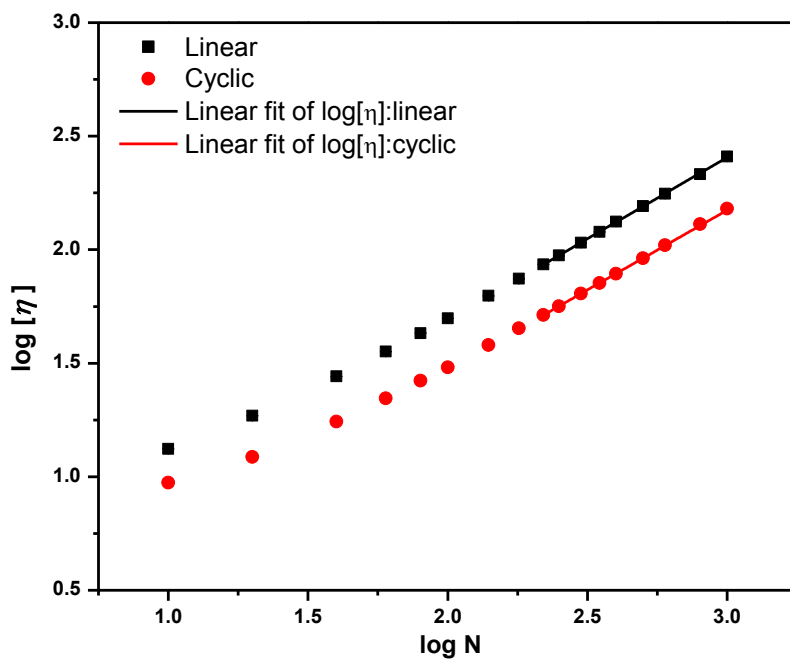


Figure S9. The dependence of the intrinsic viscosity on the number of beads. The limiting slopes of linear and cyclic polymers at high N are 0.72 and 0.70, respectively. They are in good agreement with the values of Mansfield and Douglas, 0.71^1 and 0.69^2 , respectively.



References

1. Mansfield, M.L.; Douglas, J.F., Influence of variable hydrodynamic interaction strength on the transport properties of coiled polymers. *Phys. Rev. E* **2010**, *81*, 021803.
2. Mansfield, M.L.; Douglas, J.F., Properties of knotted ring polymers. II. Transport properties. *J. Chem. Phys.* **2010**, *133*, 044904.